Electronic Supplementary Material (ESI) for Journal of Materials Chemistry A.
This journal is © The Royal Society of Chemistry 2024

Supplementary Information for

High performance of regenerated $LiFePO_4$ from spent cathodes via an in situ coating and heteroatom-doping strategy using amino acids

Junwei Wang[a,b], Shuaijing Ji[a,b], Qigao Han[b], Fengqian Wang[a,b], Wuxin Sha[b], Danpeng Cheng[b], Weixin Zhang[b], Shun Tang[b*], Yuan-Cheng Cao[b], Shijie Cheng[b]

[a] School of Materials Science and Engineering, Huazhong University of Science and Technology, Wuhan 430074, China

[b] State Key Laboratory of Advanced Electromagnetic Engineering and Technology, School of Electrical and Electronic Engineering, Huazhong University of Science and Technology, Wuhan 430074, China

*Corresponding author Email: shuntang@hust.edu.cn (S. Tang)

Computational details

All the calculations are performed in the framework of the density functional theory with the projector augmented plane-wave method, as implemented in the Vienna ab initio simulation package[1]. The generalized gradient approximation proposed by Perdew, Burke, and Ernzerhof is selected for the exchange-correlation potential[2]. The cut-off energy for plane wave is set to 400 eV. The energy criterion is set to 10^{-6} eV in iterative solution of the Kohn-Sham equation. A vacuum layer of 15 Å is added perpendicular to the sheet to avoid artificial interaction between periodic images. The Brillouin zone integration is performed using a 2x2x1 k-mesh for pyridine-N doped graphene and a 4x2x1 k-mesh for $LiFePO_4$ (010) model. All the structures are relaxed until the residual forces on the atoms have declined to less than 0.03 eV/Å.

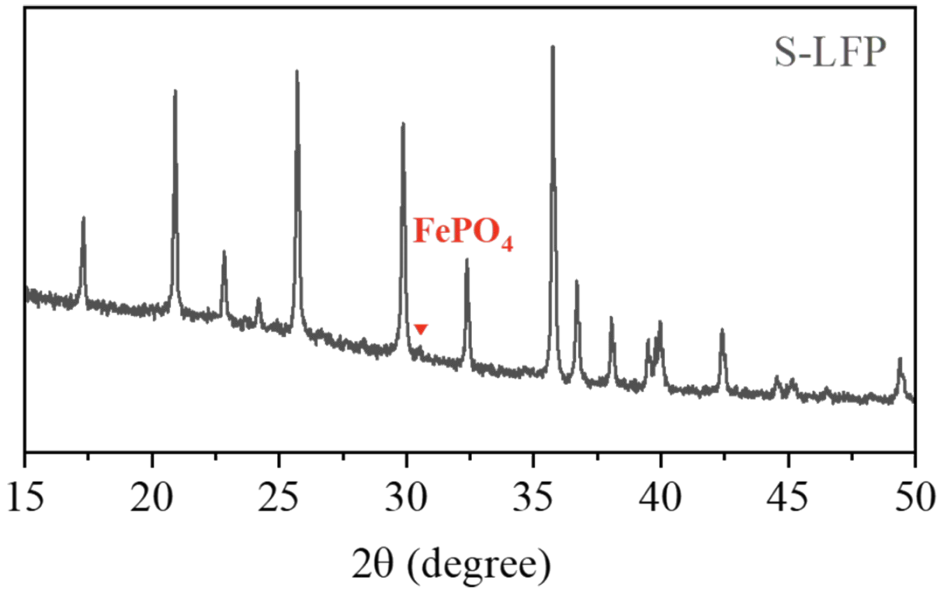

Supplementary Figure 1. The XRD pattern of S-LFP.

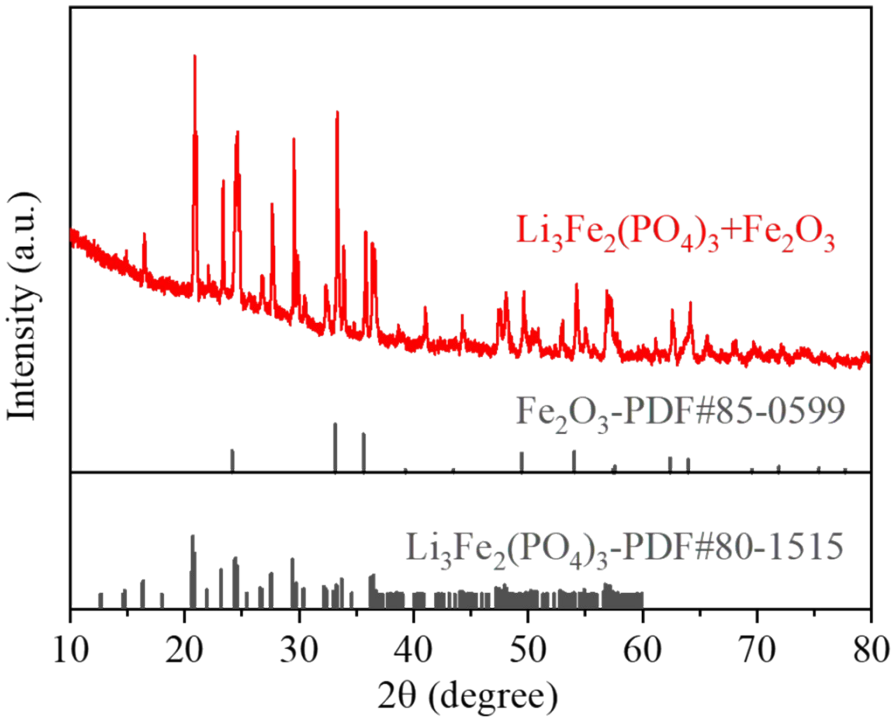

Supplementary Figure 2. The XRD pattern of oxidized S-LFP.

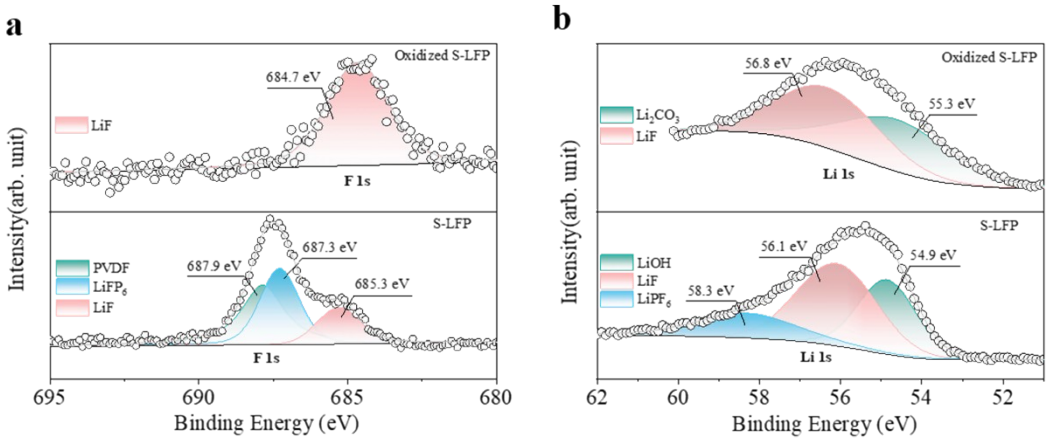

Supplementary Figure 3. a The F 1s spectrum of S-LFP and oxidized S-LFP. **b** The Li 1s spectrum of S-LFP and oxidized S-LFP.

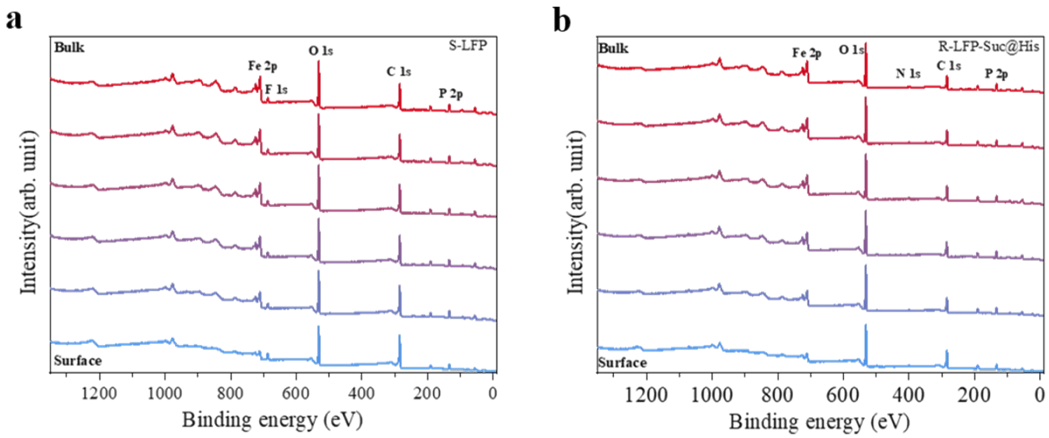

Supplementary Figure 4. a In-depth XPS survey of S-LFP. **b** In-depth XPS survey of R-LFP-Suc@His.

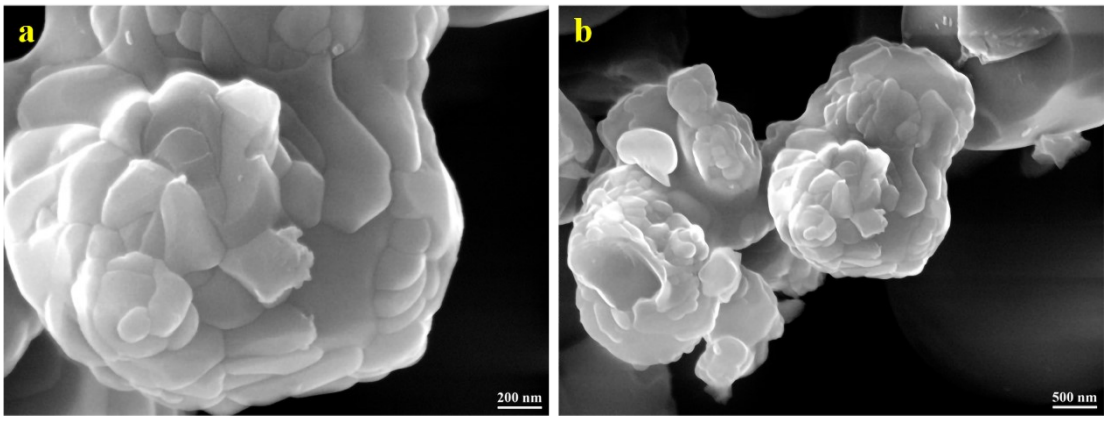

Supplementary Figure 5. a,b SEM images of oxidized S-LFP.

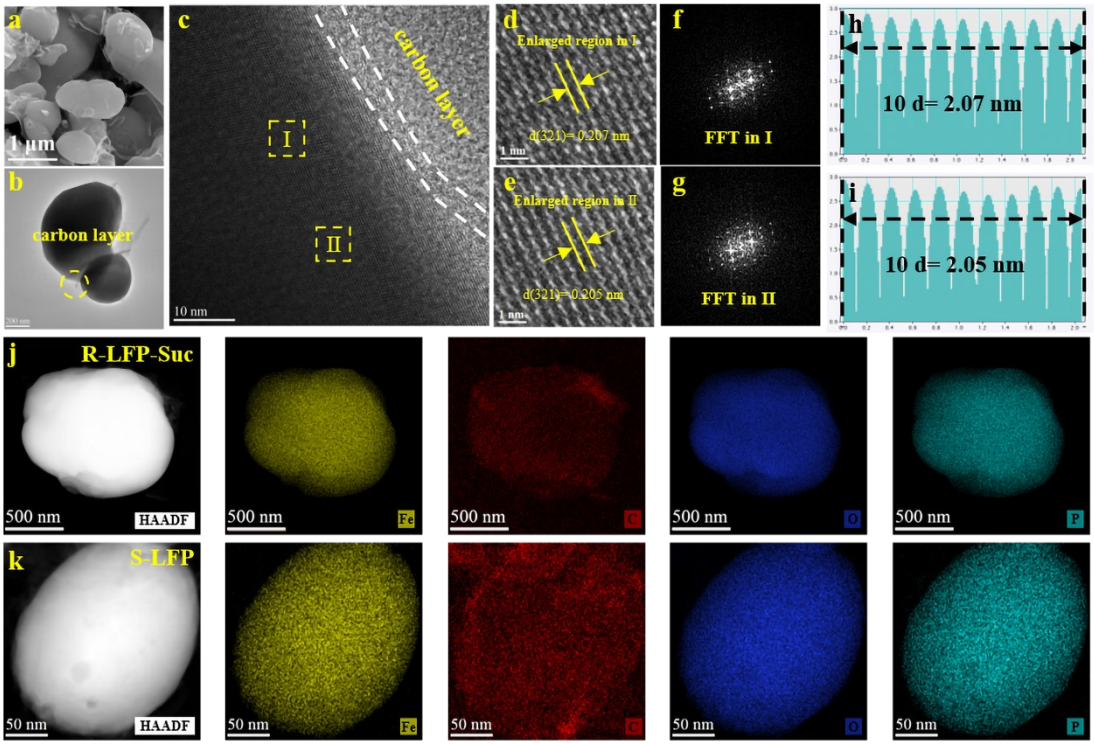

Supplementary Figure 6. a,b SEM and TEM images of R-LFP-Suc. **c** HRTEM image of R-LFP-Suc. **d,e** Enlarged figures. **f,g** Fast Fourier transform (FFT) images of region I and region II. **h,i** Line profiles in (f) and (g). **j** TEM mapping images for Fe,N,C,O and P in R-LFP-Suc. **k** TEM mapping images for Fe,N,C,O and P in S-LFP.

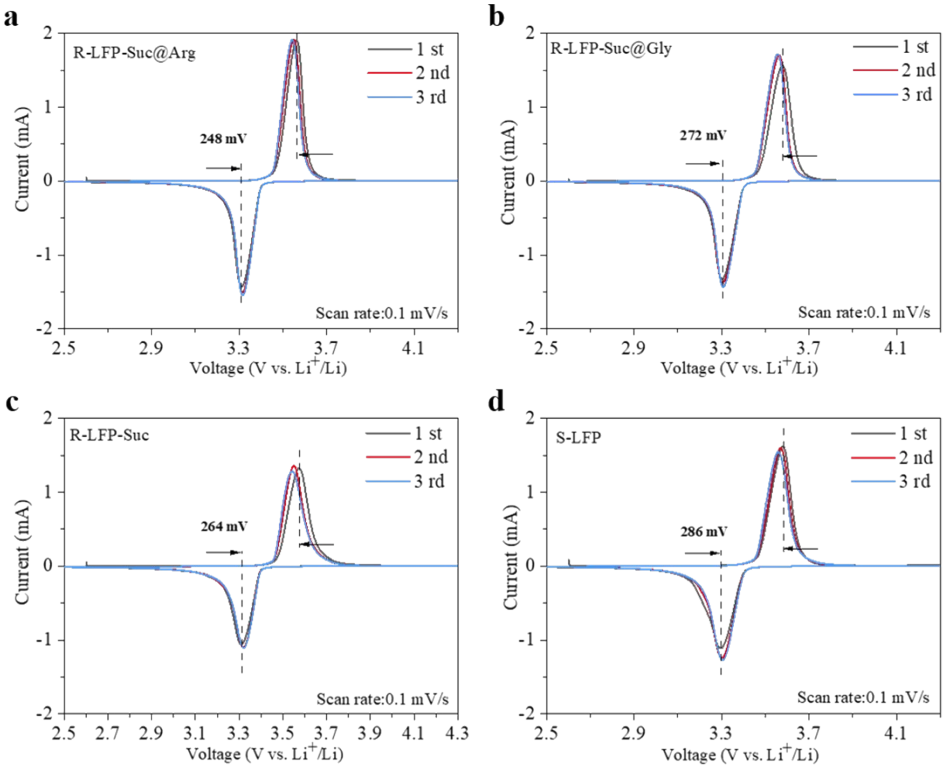

Supplementary Figure 7. The first three CV curves. **a** R-LFP-Suc@Arg. **b** R-LFP-Suc@Gly. **c** R-LFP-Suc. **d** S-LFP.

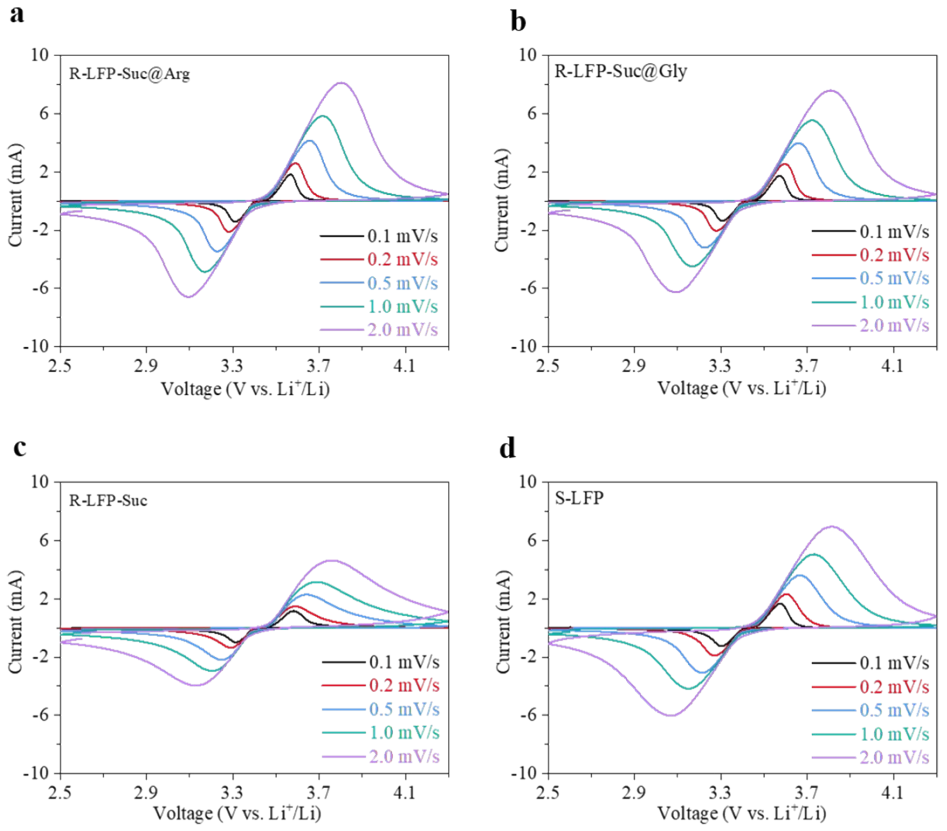

Supplementary Figure 8. CV curves of LFP at different scan rates. **a** R-LFP-Suc@Arg. **b** R-LFP-Suc@Gly. **c** R-LFP-Suc. **d** S-LFP.

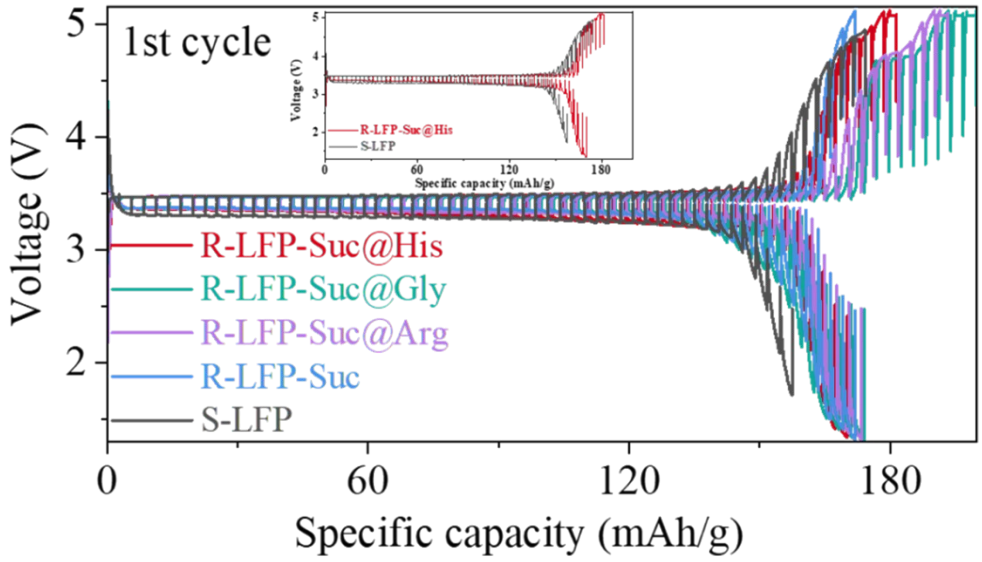

Supplementary Figure 9. GITT curves during the first cycle of S-LFP, R-LFP-Suc, R-LFP-Suc@Arg, R-LFP-Suc@Gly and R-LFP-Suc@His.

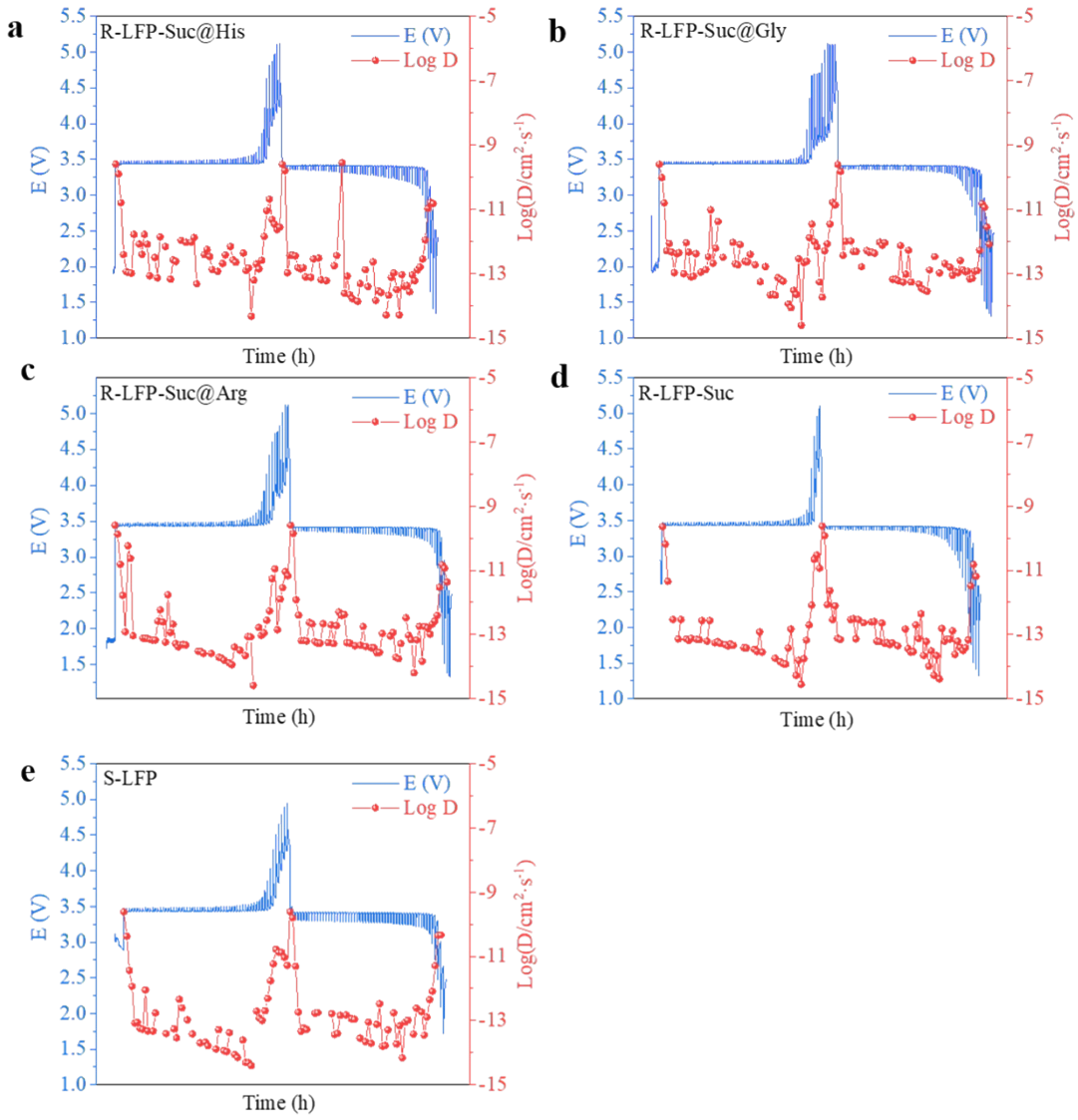

Supplementary Figure 10. GITT profiles for the discharge/charge process (blue curves) and diffusion coefficients (red curves) of **a** R-LFP-Suc@His, **b** R-LFP-Suc@Gly, **c** R-LFP-Suc@Arg, **d** R-LFP-Suc, **e** S-LFP.

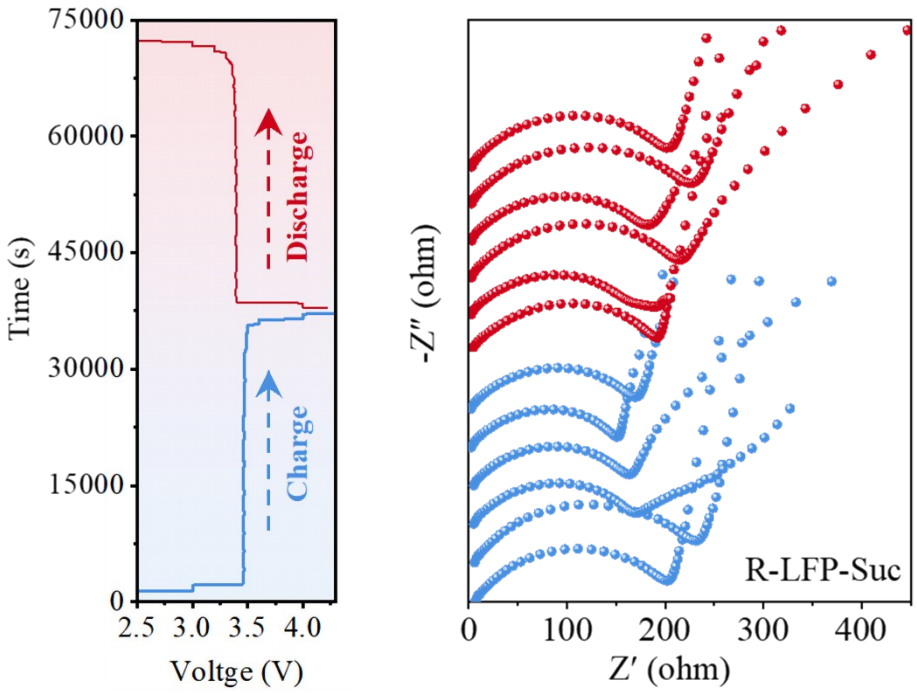

Supplementary Figure 11. In situ EIS of R-LFP-Suc during charge/discharge.

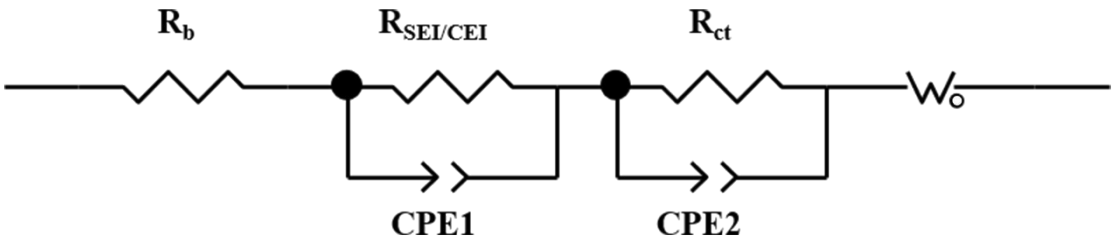

Supplementary Figure 12. Equivalent circuit model used to fit experimental EIS data .

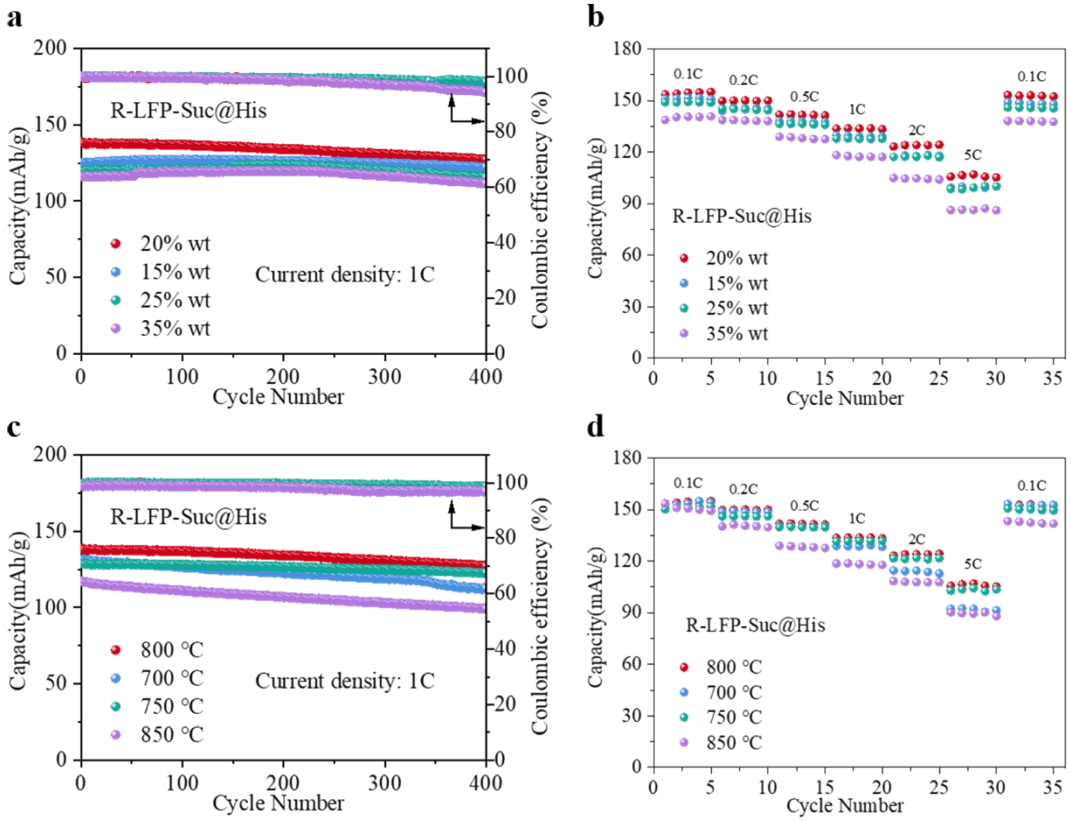

Supplementary Figure 13. a,b The cycling performance and rate performance of R-LFP-Suc@His with different sucrose contents. **c,d** The cycling performance and rate performance of R-LFP-Suc@His at different temperatures.

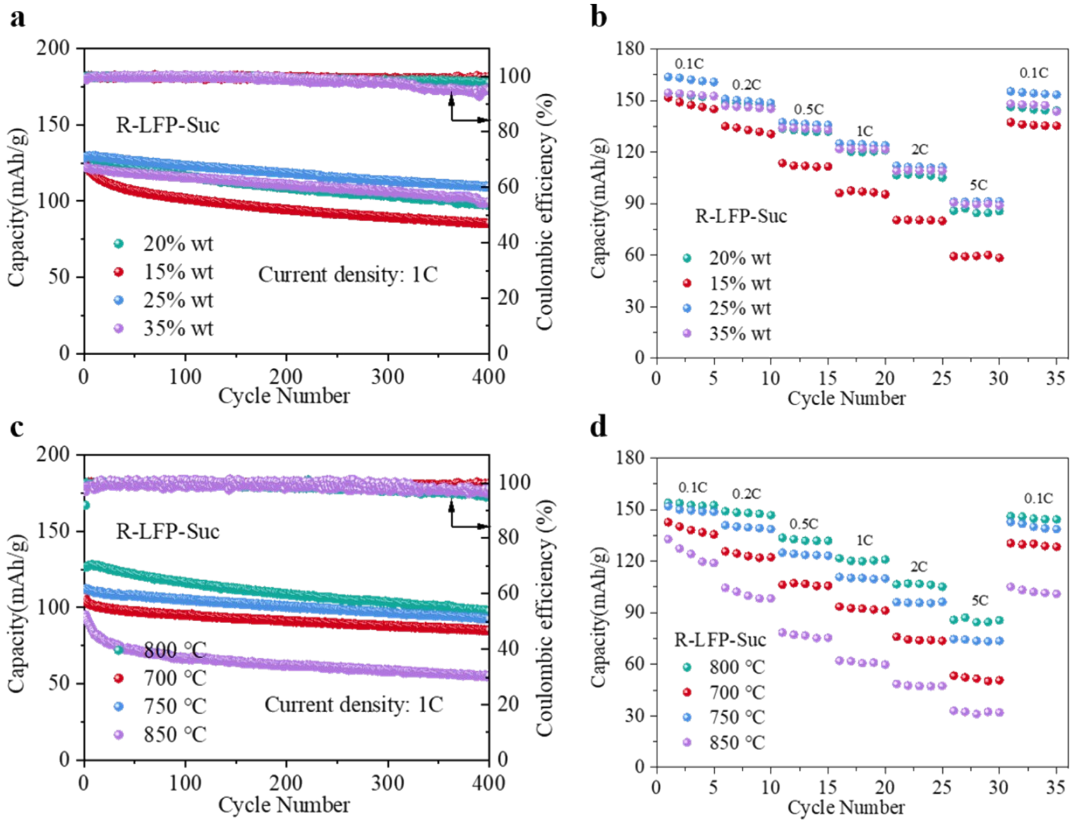

Supplementary Figure 14. a,b The cycling performance and rate performance of R-LFP-Suc with different sucrose contents. **c,d** The cycling performance and rate performance of R-LFP-Suc at different temperatures.

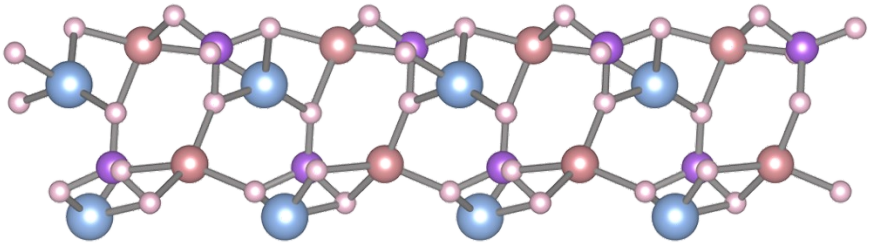

LFP (010)

Supplementary Figure 15. The optimized structure model of the LFP.

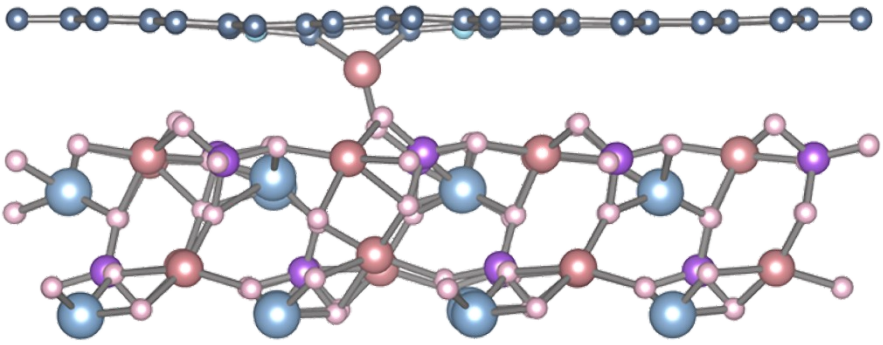

LFP (010)

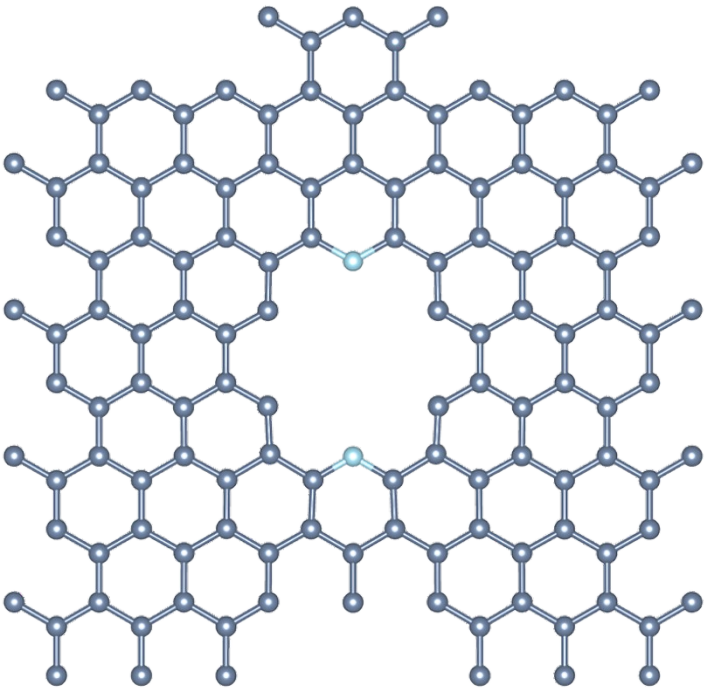

N doped carbon structure

Supplementary Figure 16. The optimized structure model of the R-LFP-Suc@His.

Supplementary Table 1. ICP-OES analysis of the powder from S-LFP, S-LFP after oxidized, S-LFP after cleaned, R-LFP-Suc@His, R-LFP-Suc@Gly, R-LFP-Suc@Arg, R-LFP-Suc.

Sample	Li (mol):Fe (mol):P (mol)	molar ratio
S-LFP		1.33:1:1
S-LFP after oxidized		1.28:1:1.01
S-LFP after cleaned		0.98:1:1.01
R-LFP-Suc@His		1.07:1:1
R-LFP-Suc@Gly		1.01:1:1.01
R-LFP-Suc@Arg		1:1:1
R-LFP-Suc		1.02:1:1

Supplementary Table 2. The carbon content of R-LFP-Suc@His and R-LFP-Suc.

Sample	Testing Quality (g)	C (wt%)
R-LFP-Suc@His	0.1012/0.2052	4.474/4.410
R-LFP-Suc	0.2070/0.2111	2.972/2.970

Supplementary Table 3. Fitting result of equivalent circuit model for impedance parameters at different state of S-LFP sample. (C-Charge, D-Discharge.)

Charge/Discharge	R_b (Ω)	R_{ct} (Ω)
C-2.5 V	1.438	132.2
C-3.0 V	1.149	120.8
C-3.5 V	1.11	82.42
C-3.6 V	1.425	77.56
C-4.0 V	1.389	58.53
C-4.3 V	1.416	54.02
D-4.0 V	1.5	68.61
D-3.4 V	1.285	71.23
D-3.3 V	1.371	69.77
D-3.2 V	1.467	83.02
D-3.0 V	1.35	90.49
D-2.5 V	1.394	118

Supplementary Table 4. Fitting result of equivalent circuit model for impedance parameters at different state of R-LFP-Suc@His sample. (C-Charge, D-Discharge.)

Charge/Discharge	R_b (Ω)	R_{ct} (Ω)
C-2.5 V	2.796	311
C-3.0 V	2.778	314.1
C-3.5 V	2.73	61.87
C-3.6 V	2.835	64.63
C-4.0 V	2.411	50.88
C-4.3 V	2.509	51.72
D-4.0 V	2.303	52.16
D-3.4 V	2.157	54.03
D-3.3 V	2.013	48.58
D-3.2 V	2.597	52.95
D-3.0 V	2.138	50.77
D-2.5 V	2.243	55.75

Supplementary Table 5. The electrochemical properties of regenerated LFP samples in previous work and this work.

Samples	Methods	Capacity (mAh/g)	Capacity retention	Ref.
S-650	Solid state sintering	147.0 mAh/g at 0.2C	95.32% after 100 cycles at 0.2C	3
S-14	Full-solid route	140.0 mAh/g at 0.2C	101.9% after 100 cycles at 0.2C	4
regenerated LFP	Hydrothermal	105.0 mAh/g at 1C	98.6% after 200 cycles at 0.2C	5
Regeneration-LFP	Solid state sintering	129.43 mAh/g at 0.5C	92.96% after 1000 cycles at 0.5C	6
R-LFP-700	Hydrothermal	145.93 mAh/g at 0.2C	99.1% after 200 cycles at 1C	7
Re-$LiFePO_4$	Fenton reaction and solid state sintering	140.0 mAh/g at 1C	91% after 200 cycles at 1C	8
RA-LFP	Hydrothermal	159.0 mAh/g at 0.5C	99% after 100 cycles at 0.5C	9
repaired $LiFePO_4$	Solid state sintering	139.0 mAh/g at 0.2C	95% after 100 cycles at 0.2C	10
R-LFP-2 h	Molten Salt	145.0 mAh/g at 0.5C	90%% after 100 cycles at 0.5C	11
regenerated $LiFePO_4$	embedding-lithium process	135.2 mAh/g at 1C	95.3% after 500 cycles at 1C	12
regenerated LFP	One-step hydrothermal	140.0 mAh/g at 1C	99% after 100 cycles at 1C	13
LFP-500	oxidation/reduction proces	141.6 mAh/g at 1C	92% after 300 cycles at 2C	14
R-LFP-Li_2DHBN	Using organic lithium salt	140.0 mAh/g at 1C	90% after 300 cycles at 1C	15
RSLFP@NC	Hydrothermal	139.0 mAh/g at 1C	99.5% after 100 cycles and 85.2% after 500 cycles at 1C	16
R-LFP-Suc@His	Redox process	138.8 mAh/g at 1C	98.7% after 100 cycles and 87.9% after 500 cycles at 1C	this work

References

1. G. Kresse and D. Joubert, *Phys. Rev. B*, 1999, **59**, 1758-1775.
2. J. P. Perdew, K. Burke and M. Ernzerhof, *Phys. Rev. Lett.*, 1997, **78**, 1396-1396.
3. X. Li, J. Zhang, D. Song, J. Song and L. Zhang, *J. Power Sources*, 2017, **345**, 78-84.
4. Q. Sun, X. Li, H. Zhang, D. Song, X. Shi, J. Song, C. Li and L. Zhang, *J. Alloys Compd.*, 2020, **818**, 153292.
5. Y. Song, B. Xie, S. Song, S. Lei, W. Sun, R. Xu and Y. Yang, *Green Chem.*, 2021, **23**, 3963-3971.
6. L. Wang, J. Li, H. Zhou, Z. Huang, S. Tao, B. Zhai, L. Liu and L. Hu, *J. Mater. Sci.: Mater. Electron.*, 2018, **29**, 9283-9290.
7. B. Chen, M. Liu, S. Cao, H. Hu, G. Chen, X. Guo and X. Wang, *J. Alloys Compd.*, 2022, **924**, 166487.
8. X. Chen, S. Li, Y. Wang, Y. Jiang, X. Tan, W. Han and S. Wang, *Waste Manage.*, 2021, **136**, 67-75.
9. P. Xu, Q. Dai, H. Gao, H. Liu, M. Zhang, M. Li, Y. Chen, K. An, Y. S. Meng, P. Liu, Y. Li, J. S. Spangenberger, L. Gaines, J. Lu and Z. Chen, *Joule*, 2020, **4**, 2609-2626.
10. Q. Liang, H. Yue, S. Wang, S. Yang, K.-h. Lam and X. Hou, *Electrochim. Acta*, 2020, **330**, 135323.
11. X. Liu, M. Wang, L. Deng, Y.-J. Cheng, J. Gao and Y. Xia, *Ind. Eng. Chem. Res.*, 2022, **61**, 3831-3839.
12. D. Peng, X. Wang, S. Wang, B. Zhang, X. Lu, W. Hu, J. Zou, P. Li, Y. Wen and J. Zhang, *Green Chem.*, 2022, **24**, 4544-4556.
13. Q. Jing, J. Zhang, Y. Liu, W. Zhang, Y. Chen and C. Wang, *ACS Sustain. Chem. Eng.*, 2020, **8**, 17622-17628.
14. Z. Zeng, P. Xu, J. Li, C. Yi, W. Zhao, W. Sun, X. Ji, Y. Yang and P. Ge, *Adv. Funct. Mater.*, 2023, DOI: 10.1002/adfm.202308671, 2308671.
15. G. Ji, J. Wang, Z. Liang, K. Jia, J. Ma, Z. Zhuang, G. Zhou and H.-M. Cheng, *Nat. Commun.*, 2023, **14**, 584.
16. K. Jia, J. Ma, J. Wang, Z. Liang, G. Ji, Z. Piao, R. Gao, Y. Zhu, Z. Zhuang, G. Zhou and H. M. Cheng, *Adv. Mater.*, 2022, **35**, 2208034.